

Langevin-dynamics simulation of relaxation in large frustrated Josephson-junction arrays

N. Grønbech-Jensen,* A. R. Bishop, F. Falo,[†] and P. S. Lomdahl

*Theoretical Division and Advanced Computing Laboratory, Los Alamos National Laboratory,
Los Alamos, New Mexico 87545*

(Received 16 January 1992)

Simulations of large two-dimensional arrays of Josephson junctions by a classical Langevin molecular-dynamics technique on the massively parallel Connection Machine 2 are reported. Long-time relaxation studies of initially random flux configurations are performed. Hierarchical scales in both time and space are revealed when the system is under the influence of thermal noise and/or spatial disorder, as well as a perpendicular magnetic field.

Modern microlithography has made Josephson-junction arrays (JJA) in the presence of a frustrating external magnetic field and/or disorder an excellent laboratory-scale¹ vehicle with which to study (a) flux-lattice structure and dynamics in weak-link arrays, thickness-modulated superconducting thin films, or even high- T_c materials (if self-consistent magnetic fields are included), and (b) the poorly understood connections between space and time in complex dynamical systems—especially “glassy” or “ $1/f$ ” regimes in time and space.^{2,3}

Recent exciting computational advances, using massively parallel architectures, have opened the possibility of simulating new dimensions of JJA, thus allowing us to visualize qualitatively the scales of hierarchical, mesoscale structures and to follow long-time molecular dynamics (MD). This permits the direct test of proposed connections between scales in time and space. Here we report results of simulations, using a Connection Machine 2 (CM-2), on square $N \times N$ arrays, with $N = 128$.

Furthermore, we report an adaptation of Langevin MD to the CM-2 architecture. This allows us to study nonlinear and nonequilibrium phenomena on a large scale, including thermal fluctuations, and without the Monte Carlo limitations of earlier studies. We have used this technique to study JJA with resistively shunted junction^{2,3} (RSJ) dynamics, including perpendicular magnetic fields, and various kinds of static disorder.

The purpose of the present report is to study *relaxation* from an initially random flux state. We wish to exhibit the multiple length and time scales involved in this relaxation, and the influence of thermal fluctuations. This noisy relaxation is controlled by the dynamics of various mesoscopic “defect” structures defined with respect to the un-

derlying ground-state flux structure. The defects, their mesoscopic collective patterns, and their dynamics control a complex macroscopic response, but are themselves microscopically controlled by the competitions producing the ground-state flux complexity. Such multiscale responses have been observed in other competing interaction systems,⁴ e.g., spin glasses, random field magnets, and weakly pinned charge-density waves, as well as noisy responses in high-temperature superconductors.⁵ Various “creep” and “stretched-exponential” regimes have been proposed,⁶ as well as phenomenological scaling theories attempting to relate spatial domain sizes with temporal scales.⁷

The Hamiltonian for the JJA takes the form^{2,3}

$$\mathcal{H} = -E_0 \sum_{i,j} [\cos(\theta_{ij} - \theta_{i-1,j} - A_{i-1,j,ij}) + \cos(\theta_{ij} - \theta_{i,j-1} - A_{i,j-1,ij})], \quad (1)$$

where θ_{ij} is the phase of the superconducting island with the discrete coordinates (i,j) of the lattice, and $A_{ij,kl} \equiv (2e/\hbar c) \int_{ij}^{kl} \mathbf{A} \cdot d\mathbf{l}$ is the integral of the vector potential from island (i,j) to a neighboring island (k,l) [see also Eq. (3)]. The critical current of a junction is given by $I_0 = (2e/\hbar)E_0$. The $A_{ij,kl}$ summed around a plaquette obeys the following relation:

$$A_{ij,i-1,j} + A_{i-1,j,i-1,j-1} + A_{i-1,j-1,i,j-1} + A_{i,j-1,i,j} = 2\pi f,$$

where the frustration $f = Ha^2/\Phi_0$ is a constant giving the average number of flux quanta $\Phi_0 = hc/2e$ of the external magnetic field H through the area a^2 of each plaquette of the array. We also introduce the fractional charge q_{ij} , obtained as the gauge-invariant phase sum around the ij th plaquette:

$$q_{ij} = (1/2\pi) [(\theta_{ij} - \theta_{i-1,j} - A_{i-1,j,ij}) \bmod \pi + (\theta_{i-1,j} - \theta_{i-1,j-1} - A_{i-1,j-1,i,j-1}) \bmod \pi + (\theta_{i-1,j-1} - \theta_{i,j-1} - A_{i,j-1,i,j}) \bmod \pi + (\theta_{i,j-1} - \theta_{i,j} - A_{i,j,i,j-1}) \bmod \pi]. \quad (2)$$

Two situations are discussed in detail below: (a) $f = \frac{1}{2}$ uniformly. In this case $q_{ij} = \pm \frac{1}{2}$: The ground state is a checkerboard pattern, and thus it is sometimes convenient to introduce the staggered order parameter $\tilde{q}_{ij} = (-1)^{(i+j)} q_{ij}$. (b) $f = \frac{1}{2}$ with static Gaussian disorder^{6,8} of the positions of the superconducting islands.

In all of the numerical experiments considered here we model *relaxation* to a prescribed equilibrium temperature of an initially random flux configuration (i.e., quenching from high temperature), with *dynamics* introduced in the RSJ model in the form^{2,3}

$$\begin{aligned} \dot{\theta}_{ij} = & \sin(\theta_{ij+1} - \theta_{ij} - A_{ij,i,j+1}) + \sin(\theta_{ij-1} - \theta_{ij} - A_{ij,i,j-1}) + \sin(\theta_{i+1,j} - \theta_{ij} - A_{ij,i+1,j}) + \sin(\theta_{i-1,j} - \theta_{ij} - A_{ij,i-1,j}) \\ & - \eta(\dot{\theta}_{ij+1} + \dot{\theta}_{ij-1} + \dot{\theta}_{i+1,j} + \dot{\theta}_{i-1,j} - 4\dot{\theta}_{ij}) + \lambda_{ij}(t), \end{aligned}$$

where the thermal noise is introduced in a classical Langevin sense: $\langle \lambda_{ij}(t) \rangle = 0$, $\langle \lambda_{ij}(t) \lambda_{kl}(t') \rangle = 2\eta G_{ij,kl}^{-1} \times T \delta(t-t')$, with the temperature T normalized to E_0/k_B , and k_B the Boltzmann constant. Time is normalized to $\tau = (C_0 \hbar / 2e I_0)^{1/2}$, $G_{ij,kl}$ is the discrete Green's function for the square lattice, the normalized dissipation is given by $\eta = (1/R)(\hbar / 2e C_0 I_0)^{1/2}$ with R the normal resistance of a junction, and C_0 is the capacitance between a superconducting island and the ground plane. As explained in Ref. 2, this choice of capacitance is appropriate to model *local* capacitance coupling of each island. Throughout this paper we have used a damping parameter of $\eta = 1$. Periodic boundary conditions are employed in currents and voltages and the following global and gauge-invariant quantity $C(t)$ is monitored in time: $C(t) = (1/N^2) \sum_{i,j} q_{ij} (q_{i+1,j} + q_{i-1,j} + q_{i,j+1} + q_{i,j-1})$. We note that gauge invariance for observable quantities must be carefully implemented, which has not typically been the case in small-system studies.

First we consider case (a), namely, $f = \frac{1}{2}$ uniformly. Figure 1 shows the global quantity $C(t)$. The initial conditions in θ_{ij} are random in all cases and normalized times up to 10^4 are included. The results are shown for various temperatures T . Here it is important to note that the transition temperature T_c for $f = \frac{1}{2}$ is $T_c \approx 0.45$,³ for $T > T_c$ long-range flux order and superconductivity are lost. $C(t)$ is displayed for a selection of temperatures in Fig. 1 to illustrate the following time dependences that we have observed.

(i) $T \ll T_c$ and short times. Here, flux creep is observed with $C(t) \sim \ln t$ albeit over a short time [see Fig. 1(a)]. We also observe from this figure that the "asymptotic" value of C first decreases as T is increased from $T \ll T_c$ and then increases again ($T \gtrsim T_c$). This can be understood as trapping into a metastable (after the initial relaxation) flux configuration at very low T because of the uniform frustration; as T is increased, thermal tunneling over the frustration barriers is allowed and C approaches closer to its $f = \frac{1}{2}$ ground-state value ($C \rightarrow -1$); at higher T (\geq frustration pinning energy) thermal randomization occurs ($C \rightarrow 0$ for $T \gg T_c$). This interpretation is supported by the final states of the time evolutions of the actual flux structures shown in Fig. 2. At low T , we indeed observe a \tilde{q}_{ij} structure which is frozen after its initial relaxation [Fig. 2(a)], but continues to slowly evolve at intermediate T [Fig. 2(b)], and is nearly random at high T [Fig. 2(c)]. Note again that the $T=0$ absolute ground state for $f = \frac{1}{2}$ is a pure checkerboard pattern in q_{ij} and thus uniform in \tilde{q}_{ij} .

(ii) *Intermediate T* ($0.3T_c \lesssim T \lesssim 0.7T_c$). Here, after the initial rapid relaxation, we observe [Fig. 1(b)] an excellent fit to a glassy stretched-exponential type of relaxation.⁷ Specifically, Fig. 1(b) shows the fit to $C(t) \sim \exp[-(t/\tau)^\beta]$, for which we find $\beta \approx 0.45$ ($T=0.2$), in good agreement with studies of other multiple time scale systems.^{6,7} Strikingly, essentially the same β value is found for the whole temperature range. Studies of actual flux structure evolution clearly illustrates the detailed domain growth mechanisms controlling this slow relaxation regime (Figs. 2). In particular, we note the interrelated roles of domain wall and vortex defects with respect

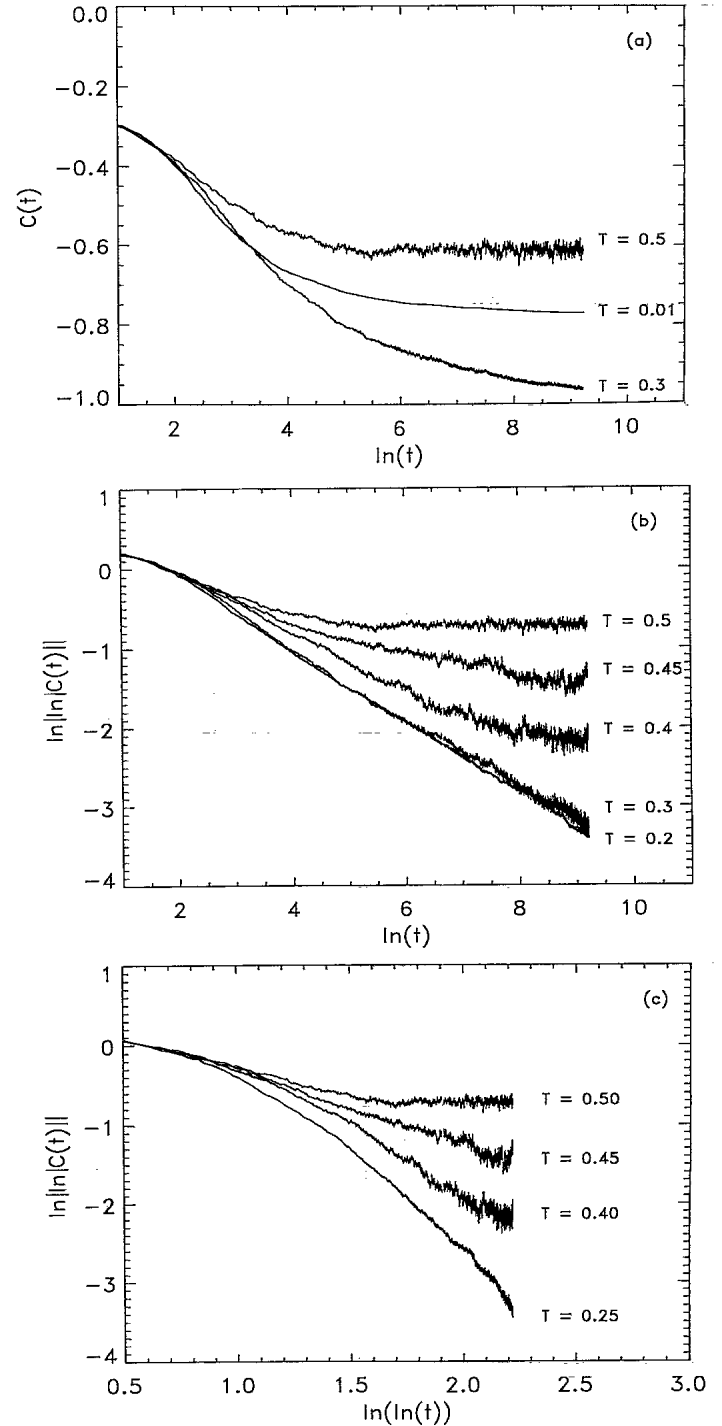


FIG. 1. Relaxation time dependence of the global correlation function $C(t)$ for frustration $f = \frac{1}{2}$ and disorder $\Delta = 0$. At $t = 0$ the flux configuration is random. (a)–(c) Results for different values of the final temperature are shown.

to the $f = \frac{1}{2}$ flux ground state. Thus, as illustrated in the sequence of snapshots shown in Fig. 3, domains typically grow by vortex-antivortex pairs nucleating, attaching to domain walls, and then counter propagating around the domain. This same growth mechanism was observed in simpler current-driven responses reported in Ref. 2.

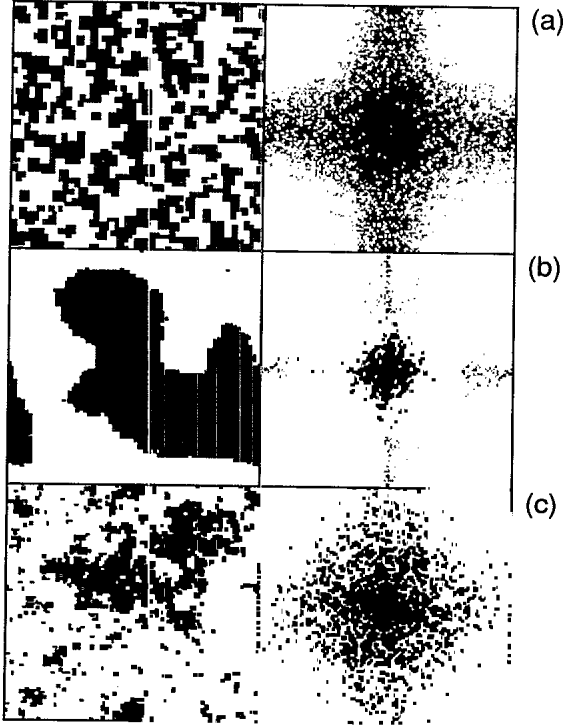


FIG. 2. The \tilde{q}_{ij} configurations (left) for a 128×128 lattice ($\tilde{q}_{ij} > 0$, black; $\tilde{q}_{ij} < 0$, white) and the spectral power $|g(\mathbf{k})|^2$ (right) at $t = 10^4$ for three different temperatures. (a) $T = 0.01$; (b) $T = 0.25$; (c) $T = 0.45$. The color code for the spectral power is $\log(|g(\mathbf{k})|^2) > 10^{-3}$, black; $10^{-5} < \log(|g(\mathbf{k})|^2) < 10^{-3}$, grey; $\log(|g(\mathbf{k})|^2) < 10^{-5}$, white.

(iii) $T \sim T_c$ (~ 0.45). Here critical effects dominate. An “activated dynamic” behavior of the form $C(t) \sim \exp(-[\ln(t/\tau)]^\delta)$ has been proposed.^{6,7} As seen in Fig. 1(c), this is in fair agreement for $T \sim T_c$, with $\delta \sim 0.9$.

(iv) $T > T_c$. Here the flux lattice melts, as illustrated in Figs. 1 and found in flux patterns (not shown).

It is of particular interest to understand the connections between many time scales and many length scales in glassy systems.^{7,9,10} Phenomenological theories based on typical clusters have been proposed, e.g., the Lifshitz-Slyozov⁷ law. The present large-scale Langevin MD approach offers the opportunity to directly probe such

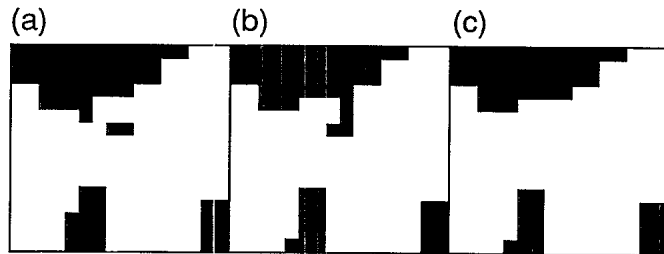


FIG. 3. Annihilation of a thermally nucleated ($T = 0.25$) vortex-antivortex pair on a domain boundary. The plots show a 16×16 section of the total 128×128 system for three different times ($t_a < t_b < t_c$, $t_c - t_a \approx 2$). As in Fig. 2 the \tilde{q}_{ij} configuration is shown by the two colors, black ($\tilde{q}_{ij} > 0$) and white ($\tilde{q}_{ij} < 0$).

phenomenologies. As an initial step, we have monitored the *spatial* Fourier transform $g(\mathbf{k})$, $\mathbf{k} = (k_x, k_y)$. This function will be sensitive to the distribution of domain sizes rather than the detailed structure of domain walls. We see in Fig. 2(c) that the disordered phase at $T > T_c$ is indeed characterized by weight on many \mathbf{k} scales, whereas the large domain structures for $T = 0.25$ in Fig. 2(b) are characterized by a few dominant \mathbf{k} scales. It will be important in the future to examine (a) whether scaling in $|j - l|$ or \mathbf{k} is observed analogous to the temporal scaling described above, and (b) whether characteristic correlation lengths scale with time, as suggested by domain phenomenologies.⁷

As noted earlier, we have also introduced various forms of *spatial* disorder, including the “vortex-glass” model⁸ with $A_{ij,kl}$ distributed independently for each link with uniform probability in $[0, 2\pi]$. This will be reported elsewhere. Here, we describe illustrative examples of Gaussian positional disorder:

$$A_{ij,kl} = 2\pi f \frac{1}{2} (x_{ij} + x_{kl})(y_{kl} - y_{ij}), \quad (3)$$

$$x_{ij} = x_{ij}^0 + \delta x_{ij}, \quad y_{ij} = y_{ij}^0 + \delta y_{ij},$$

where δx_{ij} and δy_{ij} represent the spatial disorder around the ordered positions (x_{ij}^0, y_{ij}^0) , $\langle \delta x_{ij} \rangle = \langle \delta y_{ij} \rangle = 0$,

$$\langle \delta x_{ij} \delta x_{kl} \rangle = \langle \delta y_{ij} \delta y_{kl} \rangle = \Delta \delta_{ij,kl}.$$

We might anticipate that “intermediate” strength disorder (at $T = 0$) will act somewhat like thermal fluctuations, namely, relaxation closer to the (slightly disordered) $f = \frac{1}{2}$ checkerboard ground state, whereas very weak disorder, like very low T , will lead to long-lived metastable states. Path-integral treatment of disorder fields support this view of a comparison with an effective temperature.¹¹ Higher strength disorder must, however, provide local traps for elementary vortex and domain flux defects, as well as mesoscale flux structures, inhibiting relaxation. Finally, sufficiently high strength disorder (analogous to $T > T_c$) will destroy flux order and the resulting liquidlike flux state with disorder should, at finite T , exhibit phenomena of flux localization, variable range hopping, etc.⁸

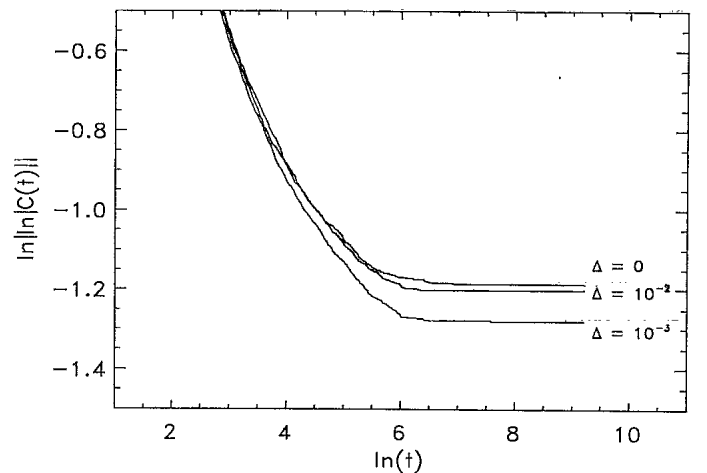


FIG. 4. Time dependences of the global correlation function $C(t)$ for $T = 0$. Three different cases of disorder Δ are shown.

Our initial studies with disorder of form (3) are consistent with this general scenario. Figure 4 shows relaxation from an initially random state for various disorder strengths. As the strength is increased from a very low value, we see the same trends as for low-intermediate temperature [Fig. 1(a)]. However, at large disorder strengths, we observe clear local pinning.

In summary, we have demonstrated a qualitative alternative capability to follow *long-time* dynamics of *large* JJA, using a realistic Langevin MD technique combined with a fine-grained massively parallel computer architecture like the CM-2. This capability is very significant for a wide range of applications, e.g., in condensed matters and materials science.¹² In the context of JJA (or related models of weak-link or even high-temperature superconductors), it allows us to explore glassy dynamics in considerable detail—namely, including and comparing effects of

spatial disorder and thermal noise, directly correlating multiple length scales with multiple time scales, and identifying the nature of specific elementary defects and mesoscopic patterns which control macroscopic responses. The simple relaxation studies reported here already illustrate each of these features, exhibiting a rich interplay of uniform frustration, temperatures and disorder, and revealing a substantial regime of stretched-exponential relaxation.

We thank the Los Alamos Advanced Computing Laboratory for generous support and for making their facilities available to us. N.G.J. is grateful to Otto Mønsted's Fond and to Carlsberg Fondet for financial support during the initial and final parts of this work, respectively. This work was performed under the auspices of the U.S. Department of Energy.

*Present address: Department of Applied Physics, Stanford University, Stanford, CA 94305.

†Permanent address: Departamento de Ciencia y Tecnología de Materiales y Fluidos, Universidad de Zaragoza, Consejo Superior de Investigaciones Científicas, Zaragoza, Spain.

¹P. Martinoli, H. Beck, M. Nsabimana, and G. A. Racine, in *Percolation, Localization and Superconductivity*, edited by A. L. Goldman and S. A. Wolf (Plenum, New York, 1984); Ch. Leeman, Ph. Lerch, G.-A. Racine, and P. Martinoli, Phys. Rev. Lett. **56**, 1291 (1986); M. Tinkham and C. J. Lobb, Solid State Phys. **42**, 91 (1989).

²F. Faló, A. R. Bishop, and P. S. Lomdahl, Phys. Rev. B **41**, 10983 (1990); N. Grønbech-Jensen, A. R. Bishop, F. Faló, and P. S. Lomdahl (unpublished).

³For example, K. K. Mon and S. Teitel, Phys. Rev. Lett. **62**, 673 (1989); J. S. Chung, K. H. Lee, and D. Stroud, Phys. Rev. B **40**, 6570 (1989); H. Eikmans and J. E. van Himbergen, *ibid.* **41**, 8927 (1990).

⁴K. Binder and A. P. Young, Rev. Mod. Phys. **58**, 801 (1986); R. Bruinsma and G. Aeppli, Phys. Rev. Lett. **52**, 1547 (1984); D. S. Fisher, Phys. Rev. B **31**, 1396 (1985).

⁵K. A. Mueller, M. Takashige, and J. G. Bednorz, Phys. Rev. Lett. **58**, 1143 (1987).

⁶I. Morgenstern, K. A. Mueller, and J. G. Bednorz, Z. Phys. B **69**, 33 (1987); R. Hetzel, M. Vanhimbeeck, and T. Schneider, *ibid.* **76**, 259 (1989); K. H. Lee and D. S. Stroud (unpublished); Yi-Hong Li and S. Teitel (unpublished).

⁷I. M. Lifshitz and V. V. Slyozov, J. Phys. Chem. Solids **19**, 35 (1961); R. G. Palmer, in *Heidelberg Colloquium on Glassy Dynamics*, edited by J. L. van Hemmen and I. Morgenstern, Lecture Notes in Physics Vol. 275 (Springer-Verlag, Berlin, 1987).

⁸For example, S. P. Benz *et al.*, Phys. Rev. B **38**, 2869 (1988); M. P. A. Fisher, T. A. Tokuyasu, and A. P. Young, Phys. Rev. Lett. **66**, 2931 (1991).

⁹C. Dekker, A. F. M. Arts, and H. W. de Wijn, Phys. Rev. B **40**, 11243 (1989); K. Gunnarsson, P. Svedlindh, P. Nordblad, and L. Lundgren, Phys. Rev. Lett. **61**, 754 (1988); P. C. Hohenberg and B. I. Halperin, Rev. Mod. Phys. **49**, 435 (1977).

¹⁰P. Bak, C. Tang, and K. Wiesenfeld, Phys. Rev. Lett. **59**, 381 (1987).

¹¹For example, G. Parisi and N. Sourlas, Phys. Rev. Lett. **43**, 744 (1979); Nucl. Phys. **B206**, 321 (1982).

¹²For example, F. Faló, A. R. Bishop, and P. S. Lomdahl, Phys. Rev. B **41**, 10983 (1990).